Image-based Object Classification of Defects in Steel using Data-driven Machine Learning Optimization

Fabian Bürger[1], Christoph Buck[2], Josef Pauli[1] and Wolfram Luther[2]
[1]*Lehrstuhl Intelligente Systeme, Universität Duisburg-Essen, Bismarckstraße 90, 47057 Duisburg, Germany*
[2]*Lehrstuhl Computergrafik und Wissenschaftliches Rechnen, Universität Duisburg-Essen, Lotharstr. 63, 47057 Duisburg, Germany*

Keywords: Object Classification, Algorithm Recommendation, Data-driven Hyper-parameter Optimization.

Abstract: In this paper we study the optimization process of an object classification task for an image-based steel quality measurement system. The goal is to distinguish hollow from solid defects inside of steel samples by using texture and shape features of reconstructed 3D objects. In order to optimize the classification results we propose a holistic machine learning framework that should automatically answer the question “How well do state-of-the-art machine learning methods work for my classification problem?” The framework consists of three layers, namely feature subset selection, feature transform and classifier which subsequently reduce the data dimensionality. A system configuration is defined by feature subset, feature transform function, classifier concept and corresponding parameters. In order to find the configuration with the highest classifier accuracies, the user only needs to provide a set of feature vectors and ground truth labels. The framework performs a totally data-driven optimization using partly heuristic grid search. We incorporate several popular machine learning concepts, such as Principal Component Analysis (PCA), Support Vector Machines (SVM) with different kernels, random trees and neural networks. We show that with our framework even non-experts can automatically generate a ready for use classifier system with a significantly higher accuracy compared to a manually arranged system.

1 INTRODUCTION

High quality steel is a versatile material that has many demanding applications such as pipeline tubes, construction and automotive engineering. In order to improve the cleanliness – the quality – of the steel, the amount of non-metallic inclusions (NMIs) inside of the product has to be reduced. These inclusions occur during the production process and usually contain materials like oxides, sulfides or nitrides.

At first, it is necessary to measure the cleanliness of steel samples to identify possible sources of contamination in the production line. Currently available measurement techniques are microscope observation, sulfur prints, SEM-scans, x-ray and ultrasonic sound analysis. Usually a high measurement precision in combination with information about the chemical composition of the NMIs is very time-consuming and therefore cost-intensive. In (Herwig et al., 2012) an automated measurement system based on optical scanning of milled steel surfaces is described. Thereby a milling machine slices thin layers of $10\mu m$ of a raw steel sample and each layer is imaged with a resolution of $2.5 – 20\mu m$ per pixel. Within these surface images, sections of different kinds of objects, namely NMIs, pores, cracks, shrink holes and milling artifacts can be found. After segmentation of the defects the binary 2D masks on consecutive layers are connected to obtain a 3D voxel-based reconstruction of the objects.

The distinction of the different object classes is crucial since only solid NMIs are relevant for the cleanliness analysis. Hollow objects like pores – which occur during treatments of the molten steel with gases (e.g. argon purging) – and cracks usually disappear after metal forming of the raw steel product. Shape features of the 3D objects in combination with machine learning can be used to classify objects into globular objects, cracks and artifacts with an accuracy of 98 – 99% (Bürger et al., 2013). At first, it was believed that all detected globular defects are solid NMIs but microscopy analyses revealed that a significant number of these objects are hollow (Buck et al., 2013). The main challenge is that solid NMIs

Bürger F., Buck C., Pauli J. and Luther W..
Image-based Object Classification of Defects in Steel using Data-driven Machine Learning Optimization.
DOI: 10.5220/0004737101430152
In *Proceedings of the 9th International Conference on Computer Vision Theory and Applications* (VISAPP-2014), pages 143-152
ISBN: 978-989-758-004-8
Copyright © 2014 SCITEPRESS (Science and Technology Publications, Lda.)

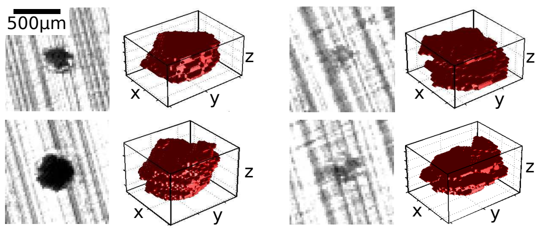

Figure 1: Texture and 3D voxels of 4 exemplary *pores*.

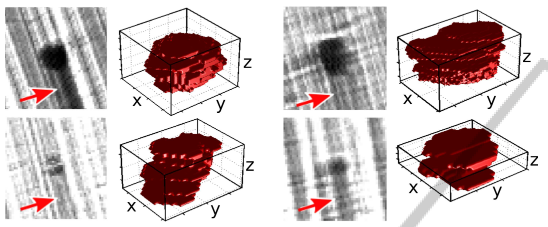

Figure 2: Texture and 3D voxels of 4 exemplary *solid NMIs*.

and hollow pores have a very similar appearance in the images of the proposed measurement system as the image resolution is at least a magnitude lower than the microscopy resolution ($\leq 1\mu m$ per pixel) used for manual verification.

The task to design a suitable classification system is difficult as it is not even known if a desired accuracy performance can be achieved with the given sensor data. First, it is not clear which texture or shape features make a distinction possible. Secondly, a suitable classifier concept with adequate parameters has to be chosen to achieve good recognition rates and generalization abilities. Additionally, dimension reduction techniques such as Principal Component Analysis may increase the performance of the system. Usually, a time-consuming development process has to be done in order to find a good classifier system. This paper targets the problem to automatically obtain such a classifier system using a holistic machine learning optimization framework which realizes a reliable image-based distinction between NMIs and pores.

2 PROBLEM DESCRIPTION

After the segmentation process a list of n_{Obj} objects is obtained and each object o_i with $1 \leq i \leq n_{Obj}$ is described with a binary voxel set $V_i(x,y,z) \in \{0,1\}$ and the 3D gray-value texture array $T_i(x,y,z) \in [0,255]$. The object size is $D_1 \times D_2 \times D_3$ and $1 \leq x \leq D_1$, $1 \leq y \leq D_2$ and $1 \leq z \leq D_3$. Example objects of pores can be found in figure 1 and objects showing NMIs are depicted in figure 2.

The variation of the object's appearance in the class NMIs is especially huge because the composition of the materials and their size are unknown. While the differences in the 3D shape are hardly noticeable, the most significant difference is the "tail" of the solid objects. It can be seen in the texture below the actual object (see arrows in figure 2). It originates from the milling cutter crushing the solid material along the milling grooves. But this tail is not clearly appearing at every NMI – hence even steel experts cannot perfectly distinguish pores from solid NMIs when only seeing their texture and shape at the system's relatively low resolution.

2.1 Machine Learning Challenges

The following steps are usually performed in a machine learning approach to distinguish objects (Jain et al., 2000). First, a set of objects is labeled from experts as ground truth. Then a set of meaningful features is derived that describes especially the differences between the classes that should be separated. Finally, a classifier is trained with the feature vectors and the ground truth labels.

Our classification task bares typical problems occurring in many machine learning applications. Due to the high cost for labeling ground truth data (in our case manual microscopic inspection) only few labels are available (72 pores and 52 solid inclusions). As it is not clear which feature set works best on the described problems, we use a set of problem-specific features combined with well-known standard descriptors which are presented in section 4.

The combination of many features is usually high-dimensional which leads to the curse of dimensionality. As only few training samples are available, high dimensional feature spaces are sampled only very sparsely and are therefore almost empty (Jain et al., 2000). Canonical distance measures, like the Euclidean distance, become less meaningful in high dimensional spaces (Beyer et al., 1999) which can lead to a degradation of classifier performance. Another effect is the negative influence of irrelevant and noisy features on the classification performance which is known as the peaking phenomenon. To overcome these dimensionality related problems, dimension reduction techniques have been proposed. The most common approaches are feature subset selection or feature transforms, such as Principal Component Analysis (PCA) (Jain et al., 2000). The feature subset selection approach removes irrelevant dimensions while a feature transform generates a compressed data representation based on the geometric properties of the original data.

The choice of a classifier concept itself determines the adaptation and generalization abilities (also called bias and variance) of the system. Many classifiers exist, such as naive Bayes classifiers, k-Nearest Neighbor classifiers (kNN), Multilayer Perceptrons (MLP), Support Vector Machines (SVM) or random trees. But there is not a single machine learning concept that performs best on all problems – this is referred to as the no-free-lunch theorem (Wolpert, 1996). Additionally, most machine learning concepts have various parameters such as kernel widths or network sizes (see section 3.3) which have a great influence on the classifier performance. In order to produce optimal results these parameters have to be tuned for each new classification problem.

2.2 Related Work

In real world machine learning tasks it is usually the case that any combination of the aforementioned problems can occur. It is time-consuming manual work to evaluate all possible combinations of solutions to achieve the optimal classifier performance. This is a general hindrance to use classifier systems in practice as each new data set, a novel feature or a different sensor may make a revision of the whole system necessary. These observations motivate a holistic view on machine learning with an automatic optimization process of the components.

In recent literature there are two categories of approaches in the context of classifier framework optimization, namely search-based and metalearning algorithms. In search algorithms, a classifier system is optimized by trying and evaluating a set of the system's hyper-parameters. Usually, the final classifier accuracy based on the training data is used as the objective function. Different search strategies and framework components have incorporated within this optimization process. In (Bergstra and Bengio, 2012) grid search and random search methods for classifier parameter optimization are compared. Furthermore, an additional feature selection component has been incorporated using genetic algorithms (Huang and Wang, 2006), particle swarms (Lin et al., 2008b) and simulated annealing (Lin et al., 2008a). In (Somorjai et al., 2004) a larger framework for biomedical spectra classification is proposed that incorporates data visualization, preprocessing, feature extraction and selection, classifier development and aggregation. The authors use several strategies to optimize the hyper-parameters and configurations. However, their approach is focused especially on the development of spectral features and interpretability in the diagnostics field.

Metalearning is an emerging field in the machine learning community and deals with the questions

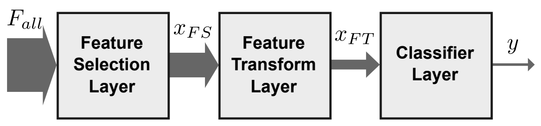

Figure 3: Overview of the layers of the proposed machine learning framework. The dimensionality is successively reduced by the feature selection and feature transform layers until the classifier returns the final one-dimensional class label y.

what knowledge can be extracted of specific learning tasks. An all-encompassing survey of this field can be found in (Lemke et al., 2013). One core aspect of metalearning is algorithm recommendation based on previous learning tasks. The idea is to establish a connection between the feature data characteristics and algorithm performance without trying all possible algorithms. In (Reif et al., 2012) a recent review of automatic classifier selection systems based on metalearning can be found. They focus on the simplicity for non-experts to automatically choose a proper classification pipeline with optimized feature selection, classifier and parameters. These approaches use meta-features of the base features to predict the performance of classifiers on the dataset. Popular meta-features contain statistical properties of the base feature vectors such as the number of samples and classes as well as entropy based distribution metrics. Furthermore, so-called landmarking features are applied as well that use the performance of very simple classifiers as a descriptor. The approach of metalearning is certainly faster than exhaustive search for the best algorithm, but it relies on the ability of meta-features to describe the "kind" of data distribution. Finally, the performance of the meta-classifier may also suffer from the same aforementioned challenges which can lead to a bad performance of the suggested algorithm on the base classification task.

3 DATA-DRIVEN MACHINE LEARNING FRAMEWORK

3.1 System Concept

In order to overcome all problems mentioned in the previous sections, we propose a data-driven and holistic machine learning framework that covers all necessary fields in machine learning, namely feature subset selection, feature transform, classifier concept, classifier parameters and evaluation with cross-validation. The coarse system structure is depicted in figure 3. The main principle of the framework is successive dimension reduction which is realized in three layers,

Table 1: Framework components on the different layers.

layer	components / algorithms
Feature Selection	dimension reduction using feature subset $F_{sub} \subseteq F_{all}$
Feature Transform	{no PCA transform, PCA with n_{PCA} dimensions}
Classifier	{naive Bayes, random tree, *k*-nearest neighbors (kNN), multilayer perceptron (MLP), Support Vector Machine (SVM) with linear and Gaussian kernel}

namely feature selection, feature transform and finally the classifier layer. Each layer contains one or more components which are listed in table 1. A system configuration is defined by the selection of one component on each layer as well as the components' specific parameters. First we describe the forward direction of the framework when the system configuration is known and a new instance should be classified. The optimization of the framework configuration can be seen as training or learning process and is described in section 3.4.

3.2 Dimension Reduction

The input for the framework is a feature group which is a set $F_{all} = \{F_1, F_2, \ldots, F_N\}$ containing N features channels. A feature channel is a vector $x_{F_i} \in \mathbb{R}^{1 \times n_i}$ with $n_i \geq 1$ dimensions. This definition allows to handle single feature values as well as higher dimensional descriptors which occur e.g. in texture features (see section 4). The concatenated feature vector of a feature group $F_{(\cdot)}$ set is defined as

$$x_{F_{(\cdot)}} = [x_{F_1}, x_{F_2}, \ldots, x_{F_N}] \in \mathbb{R}^{1 \times \hat{n}}, \quad \hat{n} = \sum_{F_i \in F_{(\cdot)}} n_i. \quad (1)$$

Note that these concatenated feature vectors could directly be used as an input for classifiers. Feature scaling should be applied to all feature channels as it improves the classifier performance (Juszczak et al., 2002). We scale the value domains to a range of $[0, 1]$. In the first layer the feature subset selection removes irrelevant features that could disturb the further process. The resulting feature subset $F_{sub} \subseteq F_{all}$ is used to form a concatenated vector x_{FS} that is passed to the feature transform layer.

Feature transforms are a powerful tool to reduce the dimensionality with estimating low dimensional manifolds inside of the high dimensional feature space. The aim is that simple classifiers (e.g. with linear kernels) may perform better on the transformed data. An overview of several common linear and non-linear techniques can be found in (Van der Maaten et al., 2009). The feature transform layer contains the Principal Component Analysis (PCA) algorithm. This is a linear transform that uses a new coordinate system whose base vectors are ordered by the highest statistical variance of the original data. The PCA can only handle linear correlations of the feature dimensions but it has been shown that it works well in many cases and allows a simple out-of-sample extension that transforms new feature vectors into the new coordinate space. If the PCA component is chosen by the framework training, the new feature vector x_{FT} is formed by using the first n_{PCA} dimensions of the PCA transformed vector of x_{FS}. Otherwise, when the PCA is deactivated, the vector x_{FS} is passed directly to the classifier and $x_{FT} = x_{FS}$.

3.3 Classifier Layer

Finally, the classifier layer contains a set of 5 popular classifier concepts which take the feature vector x_{FT} and returns a class label y for the given instance. A review of recent classifiers in machine learning can be found in (Jain et al., 2000). Table 1 lists the classifier concepts that are available in the classifier layer of our framework.

The naive Bayes classifier is based on the Bayes' theorem in combination with a Gaussian normal distribution that assigns the most probable class to an instance. This classifier has no parameters and works well for simple classification tasks.

The random tree classifier consists of a tree structure of decision nodes that check a threshold of single variables inside of the feature data.

The *k*-nearest neighbor classifier stores all feature vectors in the training phase. To classify a new instance it performs a search to find the k closest instances according to a distance metric which can be e.g. Euclidean or Mahalanobis distance. The parameter k varies the smoothness of the decision boundary.

The multilayer perceptron (MLP) is a feedforward neural network that consists of several layers which have itself a number of neurons. The layers are connected with weights that are trained using backpropagation so that the network output – the class label – matches with the input feature vector. The network size is determined by the number of hidden layers and the number of neurons per layer.

The Support Vector Machine (SVM) classifier estimates a maximum margin decision boundary in the feature vector space to minimize the risk of misclassification. It is a powerful concept that can also handle non-linear classification using kernel functions such as the Gaussian kernel. We use the ν-SVM (Chang and Lin, 2011) which has a parameter ν that penalizes misclassified instances. Furthermore, we use the linear kernel with no additional parameters as well as the Gaussian kernel with the kernel width γ that controls the smoothness of the decision boundary. Note that only one classifier is used to classify instances in a trained framework. Compared to previous frameworks we investigate the concept of the SVM with different kernels more deeply.

3.4 Training of the Framework Configuration

A framework configuration consists of the choice of active components on each layer (see table 1) as well as the choice of the corresponding parameters. The forward direction to classify a new instance is fast as only one, namely the trained configuration has to be evaluated. Clearly, it is a challenge to find the best framework configuration for a given classification problem as the number of all possible combinations is exponential and there is no straightforward way to “guess” the best configuration. Furthermore, an automatic optimization or training process is desired that does not require expert knowledge. The goal is that experts may focus on the development of better features or sensor techniques rather than time-consuming classifier optimization.

In our framework training process the only thing the user has to provide is a number of annotated ground truth instances with their feature sets. As machine learning in general is an ill-posed problem, one can describe our training approach as *totally* data-driven regularization of all system hyper-parameters. In order to find a solution in reasonable time, we propose a partly-heuristic grid search approach with the classifier performance as objective function. To define an efficient optimization strategy we use the black box principle and introduce a machine learning black box and a classifier black box which are depicted in figure 4. We separate these to use a different search strategy for each black box.

3.5 Classifier Black Box

The classifier black box (see figure 4) is the core component that optimizes the feature transform, the classifier and its parameters and evaluates the performance of the current system configuration. First, the classifier black box investigates the effect of the PCA and performs a grid search with its parameters $n_{PCA} = \{1, 2, 3, 4, 5, 10\}$. In order to save computation time, we choose this list of values as in most feature sets the intrinsic dimensionality is rather low and the first few PCA dimensions are usually sufficient. As an additional configuration, the PCA transform is

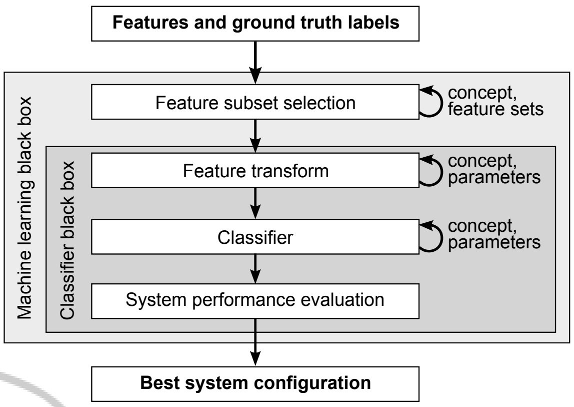

Figure 4: Black box structure for the training phase of the framework. The loop arrows on the right indicate the investigated method and parameter variations.

skipped and the feature vector x_{FS} is directly passed to the classifier. The classifier is the most important part of the classifier black box. In every round of the feature transform grid search we perform a grid search for each classifier model and its corresponding parameters that are listed in table 2. Grid search still a popular method in hyper-parameter optimization for classifiers with up to two parameters, though random search methods work better for higher dimensional search spaces (Bergstra and Bengio, 2012).

3.6 System Quality Metric

The system performance evaluation is done for each feature transform, classifier and parameter combination using k-fold cross-validation. This method achieves a good estimation of the classifiers' bias and variance at still reasonable computation costs (Jain et al., 2000). We choose $k \leq 10$ such that at least 15 samples remain in the evaluation set. The minimum size constraint for the evaluation set is necessary for small sample sizes to avoid undefined values for accuracy, precision and recall. There are several ways to define a quality metric for the whole classifier system that serves as objective function for the optimization process. It is possible to use the overall F-measure (harmonic mean of precision and recall) or e.g. the accuracy of a specific class. In many frameworks in literature (see section 2.2) the overall accuracy value is used. However, we use the average value of accuracy, precision and recall of all cross-validation rounds to reward a solution with a high value in all of the three base metrics. Precision and recall are also very important quality metrics in many classification tasks.

Table 2: Classifier concepts and parameter ranges.

classifier	**parameter ranges (steps)**
Naive Bayes	-
Random Tree (Matlab Statistics Toolbox)	- (self-optimizing with pruning)
k-nearest neighbors	$k \in [1,15](15)$, distance metric $\in$ {Euclidean, Mahalanobis}
MLP with backpropagation	number of hidden layers $\in [0,2](3)$, number of neurons per layer $\in [2,20](6)$
ν-SVM with linear kernel	$\nu \in [0.1,0.9](9)$
ν-SVM with Gaussian kernel	$\nu \in [0.1,0.9](9)$, $\gamma \in [\frac{1}{5},\frac{1}{1000}](5)$

3.7 Feature Subset Selection

The classifier black box is used to perform feature subset selection within the machine learning black box. The classifier black box is already performing feature transforms to reduce the dimensionality, but feature selection is an alternative, powerful approach to optimize the classification performance (Kohavi and John, 1997). In our experiments in section 5 we show that the performance can be significantly increased using additional feature selection. We choose wrapper approaches (rather than filters) for feature selection because the final classifier performance is used directly. As an exhaustive feature subset selection has exponential complexity with the number of features, heuristics help to efficiently decrease the computational costs. We use simple Sequential Forward and Backward Selection (SFS and SBS) as well as their more sophisticated floating extensions to find a good feature subset F_{sub}. SFS starts with an empty subset and consecutively adds the features which achieves the best quality metric when combined with the current subset. SBS starts with the full set and sequentially removes features. Sequential Floating Forward and Backward Selection (SFFS and SFBS) use these two simple strategies to obtain backtracking capabilities and achieve near-optimal solutions at reasonably higher costs (Jain et al., 2000). As each feature channel of the feature group $F_{all} = \{F_1, F_2, \ldots, F_N\}$ is not limited to one dimension (see section 4), the feature subset selection only selects whole channels to save computational time.

3.8 Training Complexity

We start with the complexity of the classifier black box optimization. Let C_i be the ith classifier of the classifier set C. The complexities of the classifier training and evaluation are denoted as $f_{\text{Train}}(\cdot)$ and $f_{\text{Eval}}(\cdot)$, respectively. Of course, they also depend on the training set and the current feature subset $\tilde{F_s}$. Using k-fold cross-validation, the complexity for a single classifier evaluation and one combination of parameters $\tilde{P}$ becomes

$$f_{\text{Param}}(C_i,\tilde{F_s},\tilde{P}) = k \cdot (f_{\text{Train}}(C_{i,\tilde{F_s},\tilde{P}}) + f_{\text{Eval}}(C_{i,\tilde{F_s},\tilde{P}})). \tag{2}$$

The classifier C_i has the set of P_i parameters and each parameter has a sampling set $P_{i,j}$ of values. Testing all parameter combinations, the Cartesian product has to be considered and the complexity for all classifiers and all of their parameters is

$$f_{\text{Classifiers}}(\tilde{F_s}) = \sum_{i=1}^{|C|} \left[\left[\prod_{j=1}^{|P_i|} |P_{i,j}| \right] \cdot f_{\text{Param}}(C_i,\tilde{F_s},\tilde{P}) \right]. \tag{3}$$

Additionally, the tier of feature transforms with n_{FT} combinations leads to a total complexity of the classifier black box of

$$f_{\text{ClassifierBlackbox}}(\tilde{F_s}) = n_{FT} \cdot f_{\text{Classifiers}}(\tilde{F_s}). \tag{4}$$

Using the classifiers and parameters of table 2 as well as the preprocessing steps, a total amount of 728 combinations is tested. As these steps are independent of each other, they can easily be parallelized.

Finally, the feature subset selection step of n_F features is performed. Testing all combinations would lead to a total complexity of $O(2^{n_F})$ and is only feasible for small feature sets. The simple selection strategies SFS and SBS have a determined number of iterations of $\frac{1}{2}(n_F^2 + n_F)$. Using floating methods the number of iterations depends on the actual quality results but is higher (though still polynomial) due to the combination of SFS and SBS.

4 OBJECT FEATURES

In order to distinguish pores from NMI objects, we derive 17 texture and shape features while the idea is to combine problem-specific features with standard state-of-the-art descriptors. The feature subset selection chooses the most promising feature subset. Therefore, the classification results most likely benefit from a large feature pool, though the computation time for the feature selection increases.

4.1 Texture Features

The tail of solid objects (described section 2) is a promising feature that we describe in the following way. First, the main direction of the milling pattern is estimated using the 2D Fourier transform. The spectrum shows a wedge shaped area of high magnitudes

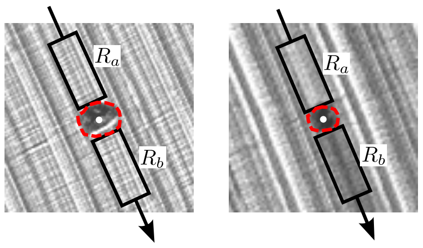

(a) Pore. (b) NMI with tail.

Figure 5: Areas for texture analysis of the tail indicator. The arrows indicate the main pattern direction. For many NMIs (b) the texture in R_b is darker than in R_a.

which can be used to robustly estimate the main angle of the pattern even in presence of noise (Herwig et al., 2012). As depicted in figure 5, two rectangular areas are defined containing the texture before (R_a) and after (R_b) the object in direction of the milling pattern. The tail indicator is calculated by dividing the average gray value inside of area R_b by the one of area R_a. This value is very close to 1 for pores and significantly lower (between 0.5 and 0.8) for NMIs with a visible tail.

Additionally, we use standard texture features, namely the mean and standard deviation of the gray values inside of the object. Local binary patterns (LBP) are a popular state-of-the-art description of textures. Generally, LBP descriptors analyze the brightness differences of a pixel and its direct neighborhood. The pattern is encoded to a binary string and aggregated to a descriptor histogram counting the frequencies of the pattern configurations. Several variants have been introduced (Doshi and Schaefer, 2012). We use the rotation invariant, uniform LBP with 8 neighbors and a radius of 1 which yields a relatively low descriptor dimension of 10 bins. We compute a histogram for each layer of the object and use the average histogram as a feature.

4.2 Shape Features

As NMI objects have different material properties than pores, their shape appears less round but more "jagged" (see figure 1 and 2). To find a proper description we use several features derived from the binary voxel array $V(x,y,z)$. The Minkowski functionals are a set of motion-invariant additive and continuous functionals which form a complete system on the set of objects that are unions of a finite number of convex bodies. A single voxel can be considered as convex body, therefore this definition can be applied to a connected voxel set like our 3D objects because it is a union of convex bodies. For the three-dimensional case the Minkowski functionals are the volume V, the surface area S, the mean curvature M (which is proportional to the mean breadth for convex particles) and the Euler number χ. Roughly speaking, the Euler number is the number of connected components minus the number of tunnels, plus the number of cavities. For the calculation of these features the reader is referred to (Buck et al., 2013). We define the density of the Minkowski functionals as a fraction of the particular functional over the total number of voxels of the minimal bounding box of the defect. Doing so we achieve a normalization of the functionals. Furthermore the densities can give interesting insights of the structure of the defects. For example the density of the surface area for a defect occupying the same volume as another defect will increase, when the surface is rougher, i.e. consists of more voxel configurations with diagonal neighbors, and approaches infinity for a fractal structure. This might be a useful feature for automatic classification. Based on the Minkowski functionals we can calculate the isoperimetric shape factors given by $f_1 = 6\sqrt{\pi}\frac{V}{\sqrt{S^3}}$, $f_2 = 48\pi^2\frac{V}{M^3}$ and $f_3 = 4\pi\frac{S}{M^2}$ which are measures for the sphericity of 3D objects. The values of f_1, f_2 and f_3 are close to 1 for spheres.

Furthermore, we derive the box dimension of the voxel set for each object. The box dimension is an empirical estimation of the upper bound of the Hausdorff dimension (Falconer, 2003). The Hausdorff dimension can be used to describe the intrinsic dimension or "porosity" of fractal objects.

We also use a voxel configuration histogram of the object border shape. In a $2 \times 2 \times 2$ neighborhood there are 256 different binary voxel configurations. The configuration can be described in a similar way to LBP using the binary string (Ohser and Mücklich, 2000)

$$\begin{aligned} g(x,y,z) = 2^0 \cdot V(x,y,z) + 2^1 \cdot V(x+1,y,z) + \\ 2^2 \cdot V(x,y+1,z) + 2^3 \cdot V(x+1,y+1,z) + \\ 2^4 \cdot V(x,y,z+1) + 2^5 \cdot V(x+1,y,z+1) + \\ 2^6 \cdot V(x,y+1,z+1) + 2^7 \cdot V(x+1,y+1,z+1). \end{aligned} \tag{5}$$

Obviously, there are 256 different values whose frequencies are – similar to LBP – stored into a histogram. This histogram can be compressed by combining symmetric cases to obtain a 22 dimensional, rotation-invariant histogram (Toriwaki and Yoshida, 2009). Another way of describing the coarseness of objects is to compute a variant of the morphological gradient. We use a 3D opening operation with a ball-shaped structuring element of radius 2 and count the additional voxels compared to the initial binary volume. To obtain a size-invariant metric, we normalize this number by the total number of voxels.

Table 3: Best classification results of the classifier black box without automatic feature selection.

Feature set	**classifier, parameters, PCA**	**accuracy / precision / recall**
only tail indicator	SVM Gauss, ν=0.5, γ=0.001, no PCA transform	0.912 / 0.899 / **0.911**
all texture features: gray-value mean, gray-value std, tail indicator, LBP histogram	SVM linear, ν=0.2, PCA, $n_{PCA} = 10$	**0.920** / **0.936** / 0.895
all shape features: volume, morphological gradient, surface area, surface density, mean breadth, Euler number (6 neighborhood), Euler number (26 neighborhood), sphericity f_1, sphericity f_2, sphericity f_3, voxel configuration 256, voxel configuration 22, box dimension	random tree, no PCA transform	0.654 / 0.653 / 0.641
all 17 features	random tree, no PCA transform	0.831 / 0.823 / 0.822

5 EXPERIMENTS AND RESULTS

5.1 Classifier Black Box Evaluation

First, we evaluate the classifier black box alone without the feature selection layer (see figure 4). We perform a “manual” feature subset selection and compare the classifier optimization results in table 3. The promising tail indicator alone already reaches an accuracy of 0.912 which shows that the tail is a key descriptor for the NMIs. The accuracy increases only slightly when the other texture features are used, too. The shape features alone perform poorly when they are concatenated. Finally, when using the simple combination of all 17 presented features, the accuracy drops significantly compared to the case when only the texture features are used. The influence of the PCA is also marginal in this scenario as it is only chosen once for the texture features. These effects indicate that some shape features contain irrelevant information that disturb the dimension reduction and classifier algorithms.

The SVM concept performs best on the texture features, but when shape features are used, the random tree classifier achieves the best results. This shows that the texture features can be separated “smoothly” and the complete set of shape features needs a rather complex decision boundary as especially the voxel configuration histograms are high-dimensional. When all 17 features are used the total feature vector space has 302 dimensions.

5.2 Feature Subset Selection

In the next experiment, all features are inside of the selection pool for the feature subset selection of the machine learning black box (see figure 4). We compare SFS, SBS and the floating versions SFFS and SFBS. The best classification results can be found in table 4. The performance increases in every case when feature selection is used. However, the results of the different selection strategies show noticeable differences. The highest performance is achieved by the SFFS selection strategy with an accuracy of 0.967. In most metrics, the forward selection strategies perform better than the backward selection algorithms. The selected subsets show a different number of items (5 – 10 features) as well as a different selection. This indicates that the subset selection strategies may get stuck in local minima, though the differences in accuracy are not extreme. The classifier concepts show that the SVM is dominating the best solutions, though its kernel parameters vary. But the MLP and the kNN classifiers appear in the top 10 result rankings, too. Here the feature transform layer has more influence and the PCA is chosen in many configurations which supports the order of our framework structure in which the feature selection is applied before the feature transform.

We can use the selected feature subsets with the top ranks (table 4 only shows rank 1) to obtain a feature relevance ranking. In table 5 the occurrences of each feature in the best 20 subsets of all selection strategies are counted. This ranking strategy is especially interesting because the feature combinations and the final classifier quality are considered. In our example, the tail indicator has been selected every time and the Minkowski functionals have also been chosen very frequently. The high dimensional histograms of the texture and the voxel configurations almost never appear in the best solutions so their usage degrades the classifier performance and should not be used.

As the theoretical complexity of the approach is relatively high, we evaluated the processing times and feature selection steps. Using an Intel Xeon CPU with 6×2.50GHz and Matlab, the average computation time for a single classifier black box optimization is 74.3 ± 38.4 seconds. The feature selection uses this

Table 4: Best classification results of the machine learning black box with different feature selection strategies.

selection strategy	selected feature subset	classifier, parameters, PCA	accuracy / precision / recall
SFS	box dimension, Euler number (6 neighborhood), sphericity f_1, sphericity f_3, surface density, tail indicator	SVM linear, ν=0.2, PCA, $n_{PCA} = 3$	0.944 / 0.953 / 0.944
SBS	box dimension, Euler number (6 neighborhood), Euler number (26 neighborhood), gray-value std, mean breadth, morphological gradient, sphericity f_3, surface density, tail indicator, volume	SVM Gauss, ν=0.3, γ=0.1, PCA, $n_{PCA} = 5$	0.943 / 0.945 / 0.946
SFFS	box dimension, Euler number (6 neighborhood), mean breadth, sphericity f_2, sphericity f_3, surface area, surface density, tail indicator, volume	SVM Gauss, ν=0.4, γ=0.001, no PCA transform	**0.967** / **0.970** / **0.962**
SFBS	mean breadth, sphericity f_2, surface density, tail indicator, volume	SVM Gauss, ν=0.3, γ=0.002, PCA, $n_{PCA} = 2$	0.952 / 0.954 / 0.953

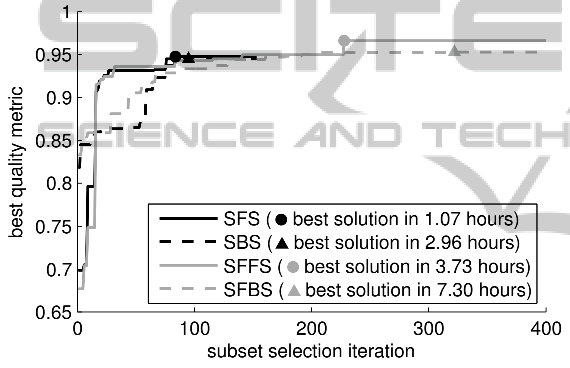

Figure 6: Progress and processing time of the classification quality depending on the subset selection strategy.

optimization and so the number of iterations needed is important. Figure 6 shows the progress of the best quality metric (see section 3.5) during the feature selection. The forward strategies (SFS and SFFS) need far less iterations to select a good subset which shows that only relatively few features are needed to solve the example classification task. Reasonably good subsets can be selected using SFS within around one hour of computation time while the fine-tuning of the SFFS needs almost 4 hours to find the overall best combination.

6 CONCLUSIONS

We presented a holistic machine learning framework that incorporates key machine learning components, namely classifier and parameters, feature transform and feature subset selection. The framework automatically optimizes the best configuration using a totally data-driven search strategy. The user just needs to provide a set of labeled ground truth feature vectors. We could successfully show the benefits of the proposed approach with an image-based object classification task. By passing feature vectors and ground truth labels, the optimization framework returns the best classifier pipeline that can be directly used. As a "byproduct" the proposed feature relevance ranking provides insight into the most distinctive descriptors of the classification problem. This knowledge can be used to develop better features. The framework can also be used as a feasibility study for classification problems to check if the measured data and the features are able to achieve a required classification accuracy. Using this framework, the machine learning component becomes a black box so that experts can focus on the development of task-specific features.

The framework uses party heuristic grid search, so the complexity of the proposed approach is relatively

Table 5: Feature relevance ranking by counting the percentaged occurrence in the top 20 results of the feature selection strategies (SFS, SBS, SFFS, SFBS).

rank	feature	%
1	tail indicator	100.00
2	surface density	97.50
3	Euler number (6 neighborhood)	80.00
4	mean breadth	71.25
5	box dimension	62.50
6	sphericity f_3	57.50
7	volume	55.00
8	sphericity f_1	52.50
9	Euler number (26 neighborhood)	47.50
10	surface area	46.25
11	gray-value std	42.50
12	sphericity f_2	33.75
13	morphological gradient	28.75
14	gray-value mean	11.25
15	LBP histogram	1.25
16	voxel configuration 256	0.00
17	voxel configuration 22	0.00

high. On the other hand, our experiments showed that it is computationally feasible on today's computer architectures for up to 20 features. The framework is in every case faster than a manual optimization by an expert. A fully exhaustive search of all feature selection combinations is clearly infeasible. Due to the huge parameter search space of the framework, e.g. evolutionary or random optimization strategies have a great potential in this approach. In future work, the framework will be applied to a larger variety of classification tasks to show its universality. Furthermore, the best classifiers can be combined to obtain an ensemble classifier (Jain et al., 2000) with a potentially greater predictive performance. Additionally, the framework can easily be extended with the newest state-of-the-art classifiers, feature transform and selection algorithms as "plugins".

REFERENCES

Bergstra, J. and Bengio, Y. (2012). Random search for hyper-parameter optimization. *J. Mach. Learn. Res.*, 13(1):281–305.

Beyer, K., Goldstein, J., Ramakrishnan, R., and Shaft, U. (1999). When is "nearest neighbor" meaningful? In Beeri, C. and Buneman, P., editors, *Database Theory ICDT99*, volume 1540 of *Lecture Notes in Computer Science*, pages 217–235. Springer Berlin Heidelberg.

Buck, C., Bürger, F., Herwig, J., and Thurau, M. (2013). Rapid inclusion and defect detection system for large steel volumes. *ISIJ International*, 53, No. 11. accepted.

Bürger, F., Herwig, J., Thurau, M., Buck, C., Luther, W., and Pauli, J. (2013). An auto-adaptive measurement system for statistical modeling of non-metallic inclusions through image-based analysis of milled steel surfaces. In Bosse, H. and Schmitt, R., editors, *ISMTII 2013, 11th International Symposium on Measurement Technology and Intelligent Instruments*. Apprimus Wissenschaftsverlag.

Chang, C.-C. and Lin, C.-J. (2011). LIBSVM: A library for support vector machines. *ACM Transactions on Intelligent Systems and Technology*, 2:27:1–27:27.

Doshi, N. and Schaefer, G. (2012). A comparative analysis of local binary pattern texture classification. In *Visual Communications and Image Processing (VCIP), 2012 IEEE*, pages 1–6.

Falconer, K. (2003). *Fractal geometry: mathematical foundations and applications*. Wiley, 2 edition.

Herwig, J., Buck, C., Thurau, M., Pauli, J., and Luther, W. (2012). Real-time characterization of non-metallic inclusions by optical scanning and milling of steel samples. In *Proc. of SPIE Vol*, volume 8430, pages 843010–1.

Huang, C.-L. and Wang, C.-J. (2006). A GA-based feature selection and parameters optimizationfor support vector machines. *Expert Systems with Applications*, 31(2):231 – 240.

Jain, A., Duin, R. P. W., and Mao, J. (2000). Statistical pattern recognition: a review. *Pattern Analysis and Machine Intelligence, IEEE Transactions on*, 22(1):4–37.

Juszczak, P., Tax, D., and Duin, R. (2002). Feature scaling in support vector data description. In *Proc. ASCI*, pages 95–102. Citeseer.

Kohavi, R. and John, G. H. (1997). Wrappers for feature subset selection. *Artificial Intelligence*, 97(12):273 – 324.

Lemke, C., Budka, M., and Gabrys, B. (2013). Metalearning: a survey of trends and technologies. *Artificial Intelligence Review*, pages 1–14.

Lin, S.-W., Lee, Z.-J., Chen, S.-C., and Tseng, T.-Y. (2008a). Parameter determination of support vector machine and feature selection using simulated annealing approach. *Applied Soft Computing*, 8(4):1505 – 1512. Soft Computing for Dynamic Data Mining.

Lin, S.-W., Ying, K.-C., Chen, S.-C., and Lee, Z.-J. (2008b). Particle swarm optimization for parameter determination and feature selection of support vector machines. *Expert Systems with Applications*, 35(4):1817 – 1824.

Ohser, J. and Mücklich, F. (2000). *Statistical analysis of microstructures in materials science*. John Wiley New York.

Reif, M., Shafait, F., Goldstein, M., Breuel, T., and Dengel, A. (2012). Automatic classifier selection for non-experts. *Pattern Analysis and Applications*, pages 1–14.

Somorjai, R. L., Alexander, M. E., Baumgartner, R., Booth, S., Bowman, C., Demko, A., Dolenko, B., Mandelzweig, M., Nikulin, A. E., Pizzi, N., Pranckeviciene, E., Summers, A. R., and Zhilkin, P. (2004). A data-driven, flexible machine learning strategy for the classification of biomedical data. In Dubitzky, W. and Azuaje, F., editors, *Artificial Intelligence Methods And Tools For Systems Biology*, volume 5 of *Computational Biology*, pages 67–85. Springer Netherlands.

Toriwaki, J. and Yoshida, H. (2009). *Fundamentals of three-dimensional digital image processing*. Springer.

Van der Maaten, L., Postma, E., and Van Den Herik, H. (2009). Dimensionality reduction: A comparative review. *Journal of Machine Learning Research*, 10:1–41.

Wolpert, D. H. (1996). The lack of a priori distinctions between learning algorithms. *Neural computation*, 8(7):1341–1390.